

Analogous Faraday effect of spin waves propagating in ferromagnetic nanotubes

Li Zhou(周利), Zhixuan Ren(任芷萱), and Ming Yan(颜明)

Citation: Chin. Phys. B, 2026, 35 (**4**): 047501. DOI: 10.1088/1674-1056/ae1ff7
http://cpb.iphy.ac.cn; http://iopscience.iop.org/cpb

What follows is a list of articles you may be interested in

Directly tunable magnon frequency comb effect based on domain wall

Xiaoxue Yang(杨霄雪), Huiting Li(李慧婷), Xue-Feng Zhang(张雪枫), Xiao-Ping Ma(马晓萍), Je-Ho Shim(沈帝虎), Yingjiu Jin(金迎九), and Hong-Guang Piao(朴红光)

Chin. Phys. B, 2025, 34 (**10**): 107507. DOI: 10.1088/1674-1056/ade856

Micromagnetic study of the dipolar-exchange spin waves in antiferromagnetic thin films

Jiongjie Wang(王炯杰) and Jiang Xiao(肖江)

Chin. Phys. B, 2025, 34 (**10**): 107505. DOI: 10.1088/1674-1056/addaa4

Magnon behavior in YIG film under microwave excitation investigated by Brillouin light scattering

Guofu Xu(徐国服), Kang An(安康), Wenjun Ma(马文俊), Xiling Li(李喜玲), C. K. Ong, Chi Zhang(张驰), and Guozhi Chai(柴国志)

Chin. Phys. B, 2025, 34 (**6**): 067507. DOI: 10.1088/1674-1056/add24c

Orbital magnetic field effect on spin waves in a triangular lattice tetrahedral antiferromagnetic insulator

Pi-Ye Zhou(周丕烨), Xiao-Hui Li(李晓慧), and Yuan Wan(万源)

Chin. Phys. B, 2025, 34 (**6**): 067501. DOI: 10.1088/1674-1056/adca1f

Skyrmion motion induced by spin-waves on magnetic nanotubes

Tijjani Abdulrazak, Xuejuan Liu(刘雪娟), Zhenyu Wang(王振宇), Yunshan Cao(曹云姗), and Peng Yan(严鹏)

Chin. Phys. B, 2024, 33 (**10**): 107504. DOI: 10.1088/1674-1056/ad5d64

SPECIAL TOPIC — Advanced magnonics

Analogous Faraday effect of spin waves propagating in ferromagnetic nanotubes

Li Zhou(周利)[†], Zhixuan Ren(任芷萱), and Ming Yan(颜明)[‡]

Physics Department, Shanghai University, Shanghai 200444, *China*

(Received 17 August 2025; revised manuscript received 16 November 2025; accepted manuscript online 17 November 2025)

We present a micromagnetic study of magnetization dynamics in ferromagnetic nanotubes. The sample is radially magnetized in equilibrium with the presence of a strong anisotropy. Micromagnetic simulations reveal that spin waves (SWs) propagating in the tube exhibit a novel effect, analogous to the well-known Faraday magneto-optic effect. Specifically, the location of the nodes/antinodes of the standing waves formed in the azimuthal direction undergoes a continuous rotation during the wave propagation under the influence of an external magnetic field. The physical mechanism is essentially the same as the Faraday effect, i.e., the breaking of the chiral symmetry by the external field. A qualitative explanation is presented by analytically solving the equation of motion of magnetization taking into account the exchange interaction. Our results may bear potential applications in the development of future spintronic devices based on SW propagation.

Keywords: spin waves, micromagnetic simulation, ferromagnetic nanotubes, chirality

PACS: 75.40.Gb, 75.30.Ds, 75.78.Cd, 75.78.–n

DOI: 10.1088/1674-1056/ae1ff7 **CSTR:** 32038.14.CPB.ae1ff7

1. Introduction

Magnonics is an emerging research field in spintronics, which aims to explore collective spin excitations (spin waves; SWs) for transmission, storage, and processing of information.[1–4] Due to the absence of Joule heat, SWs as information carriers are much more energy efficient compared to conventional charge-based carriers. This is particularly important recently due to the tremendous computing power demanded in the rapid development of machine learning and artificial intelligence.[5] In the past decades, SWs in curved magnetic structures have attracted a lot of attention, yielding some novel propagating features that do not exist in flat geometry.[6–12] A particularly interesting example is cylindrical nanowires, serving as a promising SW wave guide.[13–16] Owing to the axial symmetry, the cylindrical wire allows the existence of the so-called L and R states of SW modes, defining a chirality in the system. These two states are analogous to the two possible circular polarizations of lights in optics. It has been revealed that the seemingly identical L and R states may have different dispersion relations.[17] This dynamic chiral effect can be attributed to either the curvilinear geometry itself[11,18–21] or the presence of an asymmetric exchange interaction, i.e., the Dzyaloshinskii–Moriya interaction (DMI), in the system.[22–32] An exotic SW phenomenon, referred to as the magnonic activity, is predicted as the consequence of the splitting of the dispersion of the L and R states in cylindrical nanowires. The superposition of the L and R states results in the formation of standing waves in the azimuthal direction of the cylinder, similar to a linearly polarized light resulting from the superposition of two circularly polarized ones. During the propagation of such a SW mode, the location of the nodes/antinodes of the azimuthal standing wave undergoes a continuous rotation, just like what happens to the polarization direction of light in optical activity.[33–35]

In this paper, we report on a relevant SW effect analogous to the famous Faraday magneto-optical effect, which describes the rotation of the polarization of light in a magnetic field.[36,37] Our micromagnetic simulations show that in a radially magnetized nanotube, an external field applied in the axial direction can also cause the rotational propagation of SWs, like the the Faraday effect. A physical explanation is provided in our paper by analytically solving the equation of motion of the magnetization. It reveals that the underlying mechanism is the splitting of the dispersion of the chiral SW modes induced by the magnetic field. Furthermore, we numerically study the influence of the DMI on this effect and found that the chiral splitting and thus the rotatory power of the SW Faraday effect can be significantly enhanced by the DMI.

2. Method and materials

We study SW propagations in ferromagnetic nanotubes by micromagnetic simulations, which are performed by using the open-source package MuMax3.[38] The time evolution of the magnetization of the sample is obtained by numerically

[†]Corresponding author. E-mail: zl22720141@shu.edu.cn

[‡]Corresponding author. E-mail: myan@shu.edu.cn

© 2026 Chinese Physical Society and IOP Publishing Ltd. All rights, including for text and data mining, AI training, and similar technologies, are reserved.

solving the Landau–Lifshitz–Gilbert (LLG) equation, which is written as

$$\frac{\partial \boldsymbol{m}}{\partial t} = \gamma_0 \boldsymbol{H}_{\text{eff}} \times \boldsymbol{m} + \alpha \left[\boldsymbol{m} \times \frac{\partial \boldsymbol{m}}{\partial t} \right], \tag{1}$$

where $\boldsymbol{m} = \boldsymbol{M}/M_{\text{S}}$ is the normalized magnetization vector with M_{S} the saturation magnetization, $\gamma_0 = -\mu_0\gamma > 0$ with γ the gyromagnetic ratio, $\boldsymbol{H}_{\text{eff}}$ the effective field, and α the Gilbert damping parameter.[39] The $\boldsymbol{H}_{\text{eff}}$ term usually takes into account the external field, anisotropy, exchange, dipolar field, and DMI.

We consider a cylindrical nanotube with a length of 1200 nm, outer radius of 25 nm, and thickness of 4 nm, as shown in Fig. 1. The material of the sample is chosen to be Co/Pt,[40–42] with parameters $M_{\text{S}} = 580$ kA/m, exchange stiffness $A = 15$ pJ/m and $\alpha = 0.01$. A strong uniaxial anisotropy $Ku = 800$ kJ/m^3 is assumed with the easy axis along the radial direction of the tube. In our simulations, the sample is discretized into cubic cells with length of 1 nm.

As shown in Fig. 1, the tube is magnetized along the radial direction in equilibrium with the aid of the anisotropy. A local oscillating field is applied to stimulate SWs to propagate along the tube.

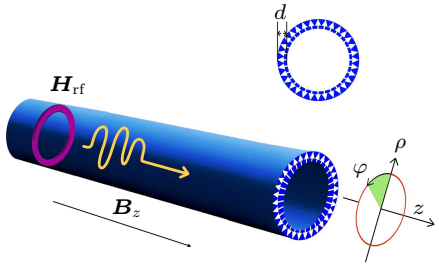


Fig. 1. Illustration of a radially magnetized ferromagnetic nanotube as a waveguide for SWs, together with a cylindrical coordinate system. An oscillating field is applied locally (at the location of the purple ring) to excite SWs (indicated by the yellow curve) to propagate along the tube.

3. Results and discussion

We demonstrate the SW profiles obtained in our simulations in Fig. 2, showing the SW Faraday effect. Here, a monochromatic mode is excited which propagates along the positive z direction. Such a mode is featured by a standing wave pattern formed in the azimuthal direction, typical for any waves travelling in a wave guide. Note that this mode can be considered as the superposition of two eigen modes of the system, the L state and the R state. Mathematically, the SW eigenstate in a nanotube can be described as $A\,\mathrm{e}^{\mathrm{i}(\omega t + n\varphi - kz)}$, where A is the amplitude, ω the angular frequency, φ the azimuthal angle, n an integer number, and k the wave number. The L and R states are characterized by negative n and positive n, respectively. These two modes correspond to the left-handed and right-handed circular polarization of light, respectively. Normally, the system possesses a chiral symmetry and the L and R states have the same dispersion relation. In this case, the wave number k is the same for the two states with the same ω. Their superposition would result in a normal standing wave pattern in the azimuthal direction. This is observed in our simulations with no external field applied in the axial direction. The wave profile of a $n = 1$ mode is illustrated in Fig. 2(a), by showing the side view of the tube (upper panel). For a better visualization, the tube is artificially "unrolled" into a flat strip (lower panel). Clearly, an expected wave pattern for waves propagating in a wave guide emerges.

In Figs. 2(b) and 2(c), the same SW mode is excited but with an external static field applied in opposite directions along the tube axis, respectively. Although the standing-wave pattern in the cross-section of the tube remains the same, the location of the node/antinode acquires a continuous rotation around the axis of the tube. Note that the direction of the rotation depends upon the direction of the field. Figure 2(d) shows the same effect occurring for a $n = 2$ mode. This phenomenon resembles the previously reported magnonic activity,[34] which also features a precessional propagation of the SWs. We nevertheless point out the difference between the two phenomena. The magnonic activity effect takes place for a longitudinally or circularly magnetized tube,[33] but not for a radially magnetized one as shown in Fig. 2(a). The SW rotation observed here is induced by an external field, which is reminiscent of the Faraday magneto-optical effect. In fact, these two wave effects in different physical scenarios possess the same physical mechanism, i.e., the breaking of the chiral symmetry.

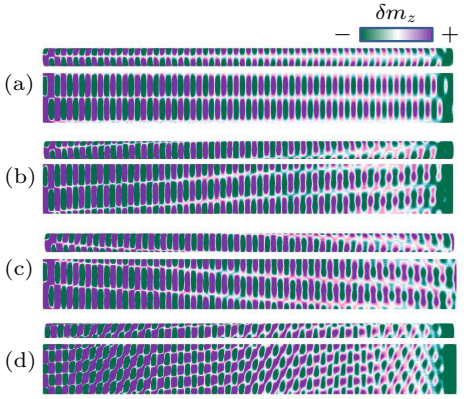


Fig. 2. Typical SW patterns in a radially magnetized nanotube obtained in micromagnetic simulations. The upper panel is the side view of the tube and the lower is the "unrolled" tube. (a) Wave profile of a $n = 1$ mode obtained in simulations without external field. (b) Wave profile of the $n = 1$ mode with an external field applied in the $+z$ direction and (c) in the $-z$ direction, showing the rotation of the standing-wave pattern formed in the azimuthal direction. (d) Wave profile of an $n = 2$ mode with an external field applied in the $+z$ direction.

In Fig. 3, we demonstrate that it is the splitting of the dispersion of the L and R states caused by the external field that is responsible for the analogous Faraday effect observed in Fig. 2. In our simulations, the L and R states with a particular order n can be excited using a specially designed rf field,

which has a profile described by $\sin(2\pi ft \mp n\varphi)$. This local field can couple to the eigen mode with frequency f and order n to the maximum. The dispersion relation of those two modes as a function of external field then can be extracted directly (Approach I in Fig. 3). The results for the $n = 1$ modes are given in Fig. 3, showing an apparent splitting between the L and R states. The dispersions of L and R states can also be calculated from the rotatory power of the superposition mode as shown in Fig. 2, which is mathematically expressed as[34]

$$\begin{aligned}\delta \boldsymbol{m}_j &= \delta \boldsymbol{m}_{j0}\left[\mathrm{e}^{\mathrm{i}(\omega t+n\varphi-k_{z1}z)}+\mathrm{e}^{\mathrm{i}(\omega t-n\varphi-k_{z2}z)}\right]\\ &= 2\delta \boldsymbol{m}_{j0}\cos\left(n\varphi-k_z'z\right)\mathrm{e}^{\mathrm{i}(\omega t-k_z''z)}, \quad j=\varphi,z, \quad (2)\end{aligned}$$

where $\delta \boldsymbol{m}_{j0}$ is the amplitude, $k_z' = \frac{k_{z1}-k_{z2}}{2}$ and $k_z'' = \frac{k_{z1}+k_{z2}}{2}$. While k_z'' characterizes the phase velocity of the wave, and k_z' is the rotatory power (angle rotated per unit length). By measuring the wave profile shown in Fig. 2, k_z' can be obtained and thus the dispersions of the L and R states (Approach II). The results calculated using approach II are also provided in Fig. 3, which match those of approach I perfectly.

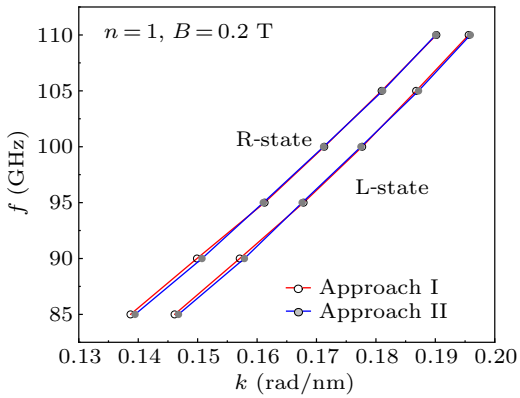


Fig. 3. The splitting of the dispersion of the R and L states of SW modes ($n = 1$) propagating in a radially magnetized nanotube, which is caused by an external field $B = 0.2$ T applied along the axial direction. The dispersion relations are obtained by extracting either from the wave profiles of the L and R states directly or from the rotation of the standing wave (superposition of the L and R states). The lines just connect the data points.

We performed a more systematic calculation of the field-induced dispersion splitting of the L and R states, with part of the results summarized in Fig. 4. It is clear that the two modes are indeed degenerate without an external field. The field-induced splitting is universal for different orders of the modes (modes with $n = 1$ and 2 are shown here). The sign of the splitting is almost completely determined by the field direction.

Figure 5 plots k_z' in Eq. (2), characterizing the rotatory power of the superposition mode, as a function of the external field for the $n = 1$ mode with three different frequencies. The data points are obtained from simulations yet the lines are linear fits. This general tendency of linear dependence of the rotatory power on the field is also similar to that of the Faraday effect. However, the ratio shows a dependence upon the mode frequency.

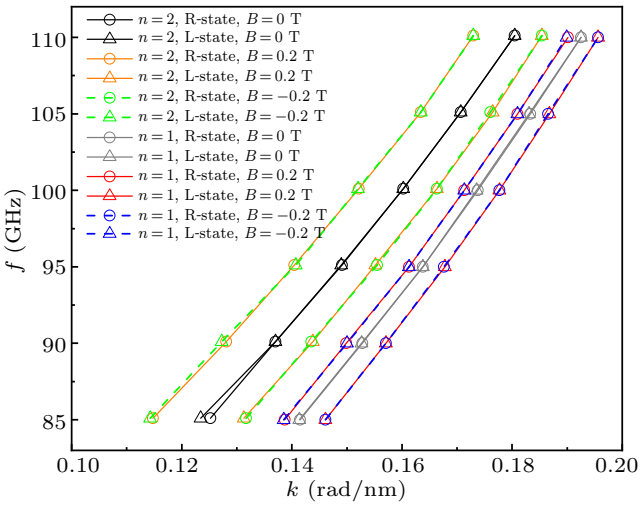


Fig. 4. Dispersion relations of the L and R states calculated from simulations for different orders ($n = 1$, 2) and different external fields ($B = 0$, 0.2 T and −0.2 T). Note that the splitting occurs for both $n = 1$ and $n = 2$ modes and the sign of the splitting depends on the direction of the field. The lines are to connect the data points.

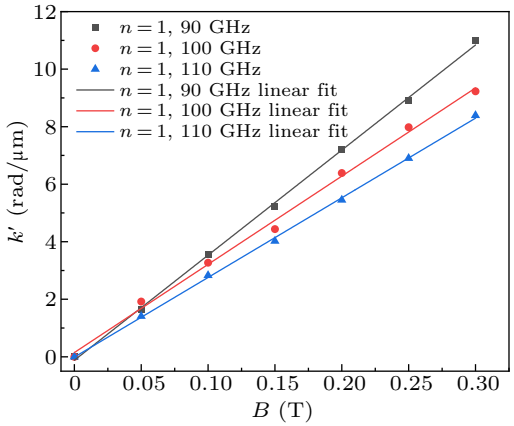


Fig. 5. The dependence of the rotational power on the external field calculated for three different frequencies. The lines are linear fits.

We now present a physical explanation to the field-induced chiral splitting observed in our simulations. Our analysis shows that it is essentially the non-vanishing axial component (z component) of the magnetization in equilibrium resulting from the external field that gives rise to the splitting.

Without an external field, the magnetization is perfectly aligned along the radial direction. With an axial field applied, the magnetization is tilted by an angle θ, hypothetically. The equilibrium magnetization thus must have two components: a radial component ($\cos\theta$) and an axial one ($\sin\theta$). In an excitation state in the linear regime, the magnetization precesses with small amplitude around the equilibrium direction, defined by θ. The dynamic magnetization for a particular SW mode then can be written as

$$\begin{aligned}\boldsymbol{m} &= \boldsymbol{m}_0+\delta\boldsymbol{m} = \cos\theta\boldsymbol{e}_\rho+\sin\theta\boldsymbol{e}_z\\ &\quad +m_1\mathrm{e}^{\mathrm{i}(\omega t+n\varphi-kz)}\boldsymbol{e}_1-\mathrm{i}m_2\mathrm{e}^{\mathrm{i}(\omega t+n\varphi-kz)}\boldsymbol{e}_2, \quad (3)\end{aligned}$$

where $\boldsymbol{e}_1 = \sin\theta\boldsymbol{e}_\rho - \cos\theta\boldsymbol{e}_z$, $\boldsymbol{e}_2 = \boldsymbol{e}_\varphi$, $\boldsymbol{m}_0 = \cos\theta\boldsymbol{e}_\rho + \sin\theta\boldsymbol{e}_z = \boldsymbol{e}_3$, and m_1 and m_2 are the oscillation amplitudes of

$\boldsymbol{e}_1$ and $\boldsymbol{e}_2$, respectively. Note that three unit vectors $\boldsymbol{e}_1$, $\boldsymbol{e}_2$, and $\boldsymbol{e}_3$ form a right-hand system. Equation (3) can be re-expressed in terms of unit vectors of a cylindrical coordinate system as

$$\begin{aligned}\boldsymbol{m} &= \boldsymbol{m}_0 + \delta\boldsymbol{m} = (\cos\theta + a\sin\theta)\boldsymbol{e}_\rho + (-\mathrm{i}b)\boldsymbol{e}_\varphi \\ &\quad + (\sin\theta - a\cos\theta)\boldsymbol{e}_z, \end{aligned} \tag{4}$$

with $a = m_1 \mathrm{e}^{\mathrm{i}(\omega t + n\varphi - kz)}$ and $b = m_2 \mathrm{e}^{\mathrm{i}(\omega t + n\varphi - kz)}$.

The dispersion relation $\omega(k)$ of the SW mode can then be calculated by substituting the expression of the dynamic magnetization into Eq. (1), neglecting the damping term. The effective field takes into account the external field $\boldsymbol{H}_{\mathrm{ext}} = \frac{B}{\mu_0}\boldsymbol{e}_z$ and the exchange field

$$\boldsymbol{H}_{\mathrm{exc}} = \frac{2\mathrm{A}}{\mu_0 M_{\mathrm{S}}}\nabla^2\boldsymbol{m} = E\nabla^2\boldsymbol{m}.$$

The solution obtained is given by

$$\omega = \frac{G - KH - \sqrt{(KH - G)^2 + 4H\,(GK - IJ)}}{-2H}, \tag{5}$$

with the parameters defined as

$$\begin{aligned} G &= 2\gamma_0 E \frac{\mathrm{i}}{\rho^2} n\sin\theta, \\ H &= -\mathrm{i}, \\ I &= \gamma_0 E\left(\frac{\mathrm{i}n^2}{\rho^2} + \mathrm{i}k^2 + \frac{\mathrm{i}}{\rho^2}\right) + \mathrm{i}\gamma_0 E\left(\frac{-1}{\rho^2}\cos^2\theta\right), \\ J &= \gamma_0 E\left(\frac{1}{\rho^2}n^2 + k^2\right) + \gamma_0 E\frac{1}{\rho^2}(\sin^2\theta - \cos^2\theta), \\ K &= \gamma_0 E\left(\frac{2n}{\rho^2}\right)\sin\theta. \end{aligned} \tag{6}$$

We first consider the situation without the external field, which means $\theta = 0$. Obviously, the dispersion relation is independent of the sign of n in this case, yielding the degeneracy of the L and R modes for a perfectly radially magnetized tube. When an external field is applied, θ assumes a nonzero value. Note that the expression of the square root on the right side of Eq. (5) only contains the terms of n^2. We focus on the rest part, which is given by

$$\frac{G - KH}{-2H} = \gamma_0 E\frac{2n}{\rho^2}\sin\theta, \tag{7}$$

which clearly leads to the splitting of the dispersion relation of the L and R modes. The sign of θ depends on the direction of the field. We choose θ to be positive when the external field is applied along the positive z direction. In this case, an R mode (n is positive) would have a greater frequency than the L mode (n is negative) for a same wave number k. The mode splitting reverses correspondingly when the external field is reversed. Also note from Eq. (7) that the size of the splitting is proportional to n. This means the splitting gets more significant for higher order modes. All those features interpreted from Eq. (5) are consistent with our simulation results discussed above.

The analytical model predicts a frequency difference, which is about 6 GHz, between the L and R modes ($n = 1$) in our system, while the simulations yield a difference in the range of 3–4 GHz as shown in Fig. 4. This discrepancy can be mainly attributed to two reasons. The first is the negligence of the dipolar interaction in our analytical model. The second is the negligence of the finite thickness (4 nm in simulations) effect. The negligence of the dipolar interaction is, to a certain extent, justified since the spin-wave frequency in our study is relatively high (around 100 GHz), making the exchange interaction dominant.

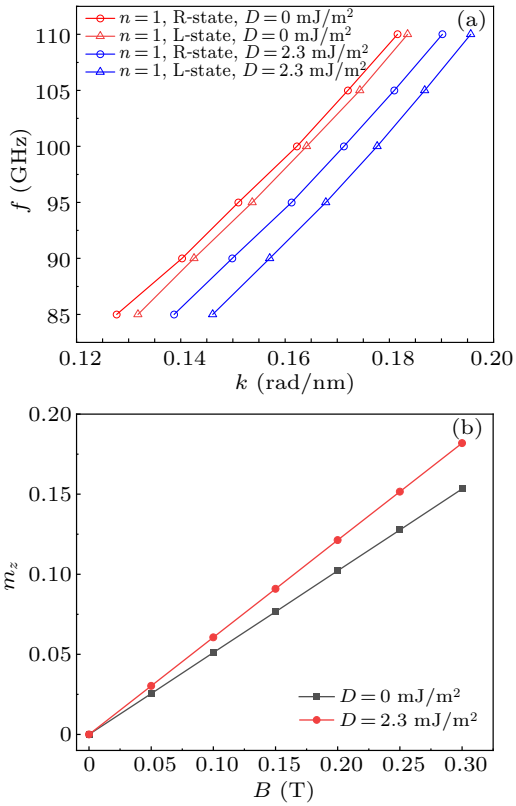


Fig. 6. (a) Influence of DMI on the dispersion splitting of the L and R states. Clearly, the splitting is enhanced with the presence of DMI in the system. (b) The influence of DMI on the equilibrium magnetization configuration of the tube obtained in simulations, yielding a larger axial component of the magnetization m_z compared to the case with no DMI.

Finally, we discuss the influence of DMI on the SW propagation in our system. Our simulations show that the presence of a DMI could cause a significant enhancement of the dispersion splitting of the L and R states. This is demonstrated in Fig. 6(a), which compares the splitting of the two $n = 1$ modes with different handedness with or without DMI. The increase of the splitting is attributed to the increase of the tilting angle θ of the equilibrium magnetization induced by DMI, as shown in Fig. 6(b). According to Eq. (7), the mode splitting is directly proportional to θ ($\sin\theta \approx \theta$ when θ is small). Therefore, DMI provides an effective way of manipulating the mode

splitting, and thus the rotatory power of the resulting standing-wave modes in our system.

4. Summary

We study the propagating properties of SWs in a radially magnetized nanotube. Micromagnetic simulations demonstrate an SW effect analogous to the Faraday magneto-optical effect. This phenomenon results from the chiral symmetry breaking induced by a static field. A theoretical model is provided which explains all the features observed in numerical calculations. Our results basically suggest a new manner that an external field impacts on the propagation of SWs in cylindrical nanowires, which could be valuable for the design of novel magnonic devices.

Acknowledgement

This research was funded by the National Natural Science Foundation of China (Grant Nos. 11774218 and 11701358).

References

[1] Bloch F 1930 *Z. Phys.* **61** 206
[2] Chumak A V, Vasyuchka V I, Serga A A and Hillebrands B 2015 *Nat. Phys.* **11** 453
[3] Cornelissen L J, Liu J, Duine R A, Youssef J B and Van Wees B J 2015 *Nat. Phys.* **11** 1022
[4] Liu C, Chen J, Liu T, Heimbach F, Yu H, Xiao Y, Hu J, Liu M, Chang H, Stueckler T, Tu S, Zhang Y G, Zhang Y, Gao P, Liao Z, Yu D, Xia K, Lei N, Zhao W and Wu M 2018 *Nat. Commun.* **9** 738
[5] Fleblus B, *et al.* 2024 *J. Phys.: Condens. Matter* **36** 363501
[6] Sheka D D, Kravchuk V P and Gaidiei Y 2015 *J. Phys. A: Math. Theor.* **48** 125202
[7] Tijjani Abdulrazak, *et al.* 2024 *Chin. Phys. B* **33** 107504
[8] Tijjani Abdulrazak, *et al.* 2024 *Chin. Phys. B* **33** 087503
[9] Xia H, Chen J, Zeng X and Yan M 2016 *Phys. Rev. B* **93** 140410
[10] Hertel R 2013 *Spin* **3** 1340009
[11] Otálora J A, Yan M, Schultheiss H, Hertel R and Kákay A 2016 *Phys. Rev. Lett.* **117** 227203
[12] Li N, Fan M, Zeng X and Yan M 2024 *Symmetry* **16** 1336
[13] Kruglyak V V, Hicken R J, Kuchko A N and Gorobets V Y 2005 *J. Appl. Phys.* **98** 014304
[14] Jia C L, Ma D C, Schaffer A F and Berakdar J 2019 *Nat. Commun.* **10** 2077
[15] Jiang Y Y, Yuan H Y, Li Z X, Wang H Y, Zhang H W, Cao Y S and Yan P 2020 *Phys. Rev. Lett.* **124** 217204
[16] Rychły J, Tkachenko V S, Kłos J W, Kuchko A and Krawczyk M 2019 *J. Phys. D: Appl. Phys.* **52** 075003
[17] Hecht E 2002 *Optics* (San Francisco: Addison Wesley)
[18] Yan M, Andreas C, Kákay A, García-Sánchez F and Hertel R 2011 *Appl. Phys. Lett.* **99** 122505
[19] Otálora J A, López-López J A, Landeros P, Vargas P and Núñez A S 2013 *J. Magn. Magn. Mater.* **341** 86
[20] Otálora J A, Yan M, Schultheiss H, Hertel R and Kákay A 2017 *Phys. Rev. B* **95** 184415
[21] Otálora J A, Kákay A, Lindner J, Schultheiss H, Thomas A, Fassbender J and Nielsch K 2018 *Phys. Rev. B* **98** 014403
[22] Dzyaloshinsky I 1958 *J. Phys. Chem. Solids* **4** 241
[23] Moriya T 1960 *Phys. Rev.* **120** 91
[24] Di K, Zhang V L, Lim H S, Ng S C, Kuok M H, Yu J, Yoon J, Qiu X and Yang H 2015 *Phys. Rev. Lett.* **114** 047201
[25] Tanigaki T, Shibata K, Kanazawa N, Yu X, Onose Y, Park H S, Shindo D and Tokura Y 2015 *Nano Lett.* **15** 5438
[26] Moon J H, Seo S M, Lee K J, Kim K W, Ryu J, Lee H W, McMichael R D and Stiles M D 2013 *Phys. Rev. B* **88** 184404
[27] Cortés-Ortuño D and Landeros P 2013 *J. Phys.: Condens. Matter* **25** 156001
[28] Guo J, Zeng X and Yan M 2017 *Phys. Rev. B* **96** 014404
[29] Xia J, Zhang X, Yan M, Zhao W and Zhou Y 2016 *Sci. Rep.* **6** 25189
[30] Wang Z, Zhang B, Cao Y and Yan P 2018 *Phys. Rev. Appl.* **10** 054018
[31] Mulkers J, Van Waeyenberge B and Milošević M V 2018 *Phys. Rev. B* **97** 104422
[32] Wang Z, Cao Y and Yan P 2019 *Phys. Rev. B* **100** 064421
[33] Yang M, Zeng X and Yan M 2022 *Symmetry* **14** 1771
[34] Yang M, Yin B, Li Z, Zeng X and Yan M 2021 *Phys. Rev. B* **103** 094404
[35] Li Z, Yang M, Fan M, Zeng X and Yan M 2024 *Spin* **14** 2450013
[36] Haider T 2017 *Int. J. Electromagn. Appl.* **7** 17
[37] Zhan J, Wang Y, Wang X, *et al.* 2024 *Chin. Phys. B* **33** 107505
[38] Vansteenkiste A, Leliaert J, Dvornik M, Helsen M, Garcia-Sanchez F and Van Waeyenberge B 2014 *AIP Adv.* **4** 107133
[39] Gilbert T L 2004 *IEEE Trans. Magn.* **40** 3443
[40] Sampaio J, Cros V, Rohart S, Thiaville A and Fert A 2013 *Nat. Nanotechnol.* **8** 839
[41] Xie K and Sang H 2014 *J. Appl. Phys.* **116** 223901
[42] Bao B, Yang M and Yan M 2022 *Symmetry* **14** 1195